ION-HOSE INSTABILITY IN A LONG-PULSE ACCELERATOR

T. P. Hughes* and T. C. Genoni, MRC, Albuquerque, NM 87110

Abstract

The ion-hose instability is a transverse electrostatic instability which occurs on electron beams in the presence of a low-density ion channel. In the DARHT-2 accelerator, the 2 kA, 2 microsecond beam pulse produces an ion channel through impact ionization of the residual background gas ($\approx\ 1.5 \times 10^{-7}$ torr average). A calculation of the linear growth by R. J. Briggs indicated that the instability could be strong enough to affect the radiographic application of DARHT, which requires that transverse oscillations be small compared to the beam radius. We present semi-analytical theory and 3-D particle-in-cell simulations (using the LSP code) of the linear and nonlinear growth of the instability, including the effects of the temporal change in the ion density, spatially decreasing beam radius etc. We find that the number of e-foldings for a particular beam slice is given approximately by the analytic expression for a uniform channel using an average value for the channel density. Hence, in the linear regime, the number of e-foldings increases linearly from head to tail of the beam pulse. We also find that growth is suppressed by nonlinear effects at relatively small amplitudes of the electron beam. This is because the ion oscillation amplitude is several times larger than that of the beam, allowing nonlinear effects to come into play.

1 INTRODUCTION

The DARHT-2 linear induction accelerator [1] is designed to produce a 2 kA, 20 MV, 2 μs flat-top electron beam. It is expected that electron impact ionization of the residual background gas in the accelerator ($\approx\ 1.5 \times 10^{-7}$ torr average) will result in a fractional electrical neutralization of the order of 10^{-4}. Even at this relatively low ion density, potentially troublesome coherent transverse displacements (ion-hose oscillations) of the beam and channel can result due to their mutual electrostatic restoring forces. In this paper, semi-analytical theory and 3-D particle-in-cell (PIC) simulation are used to investigate the potential severity of unstable ion-hose oscillations in DARHT-2. In Section 2, Lee's "spread-mass" model [2], as applied previously to the ion-hose instability [3], is extended to include the effects of a focusing magnetic field. The growth of the instability for typical DARHT-2 parameters is calculated from the linear theory, and we also make use of a convenient nonlinear ansatz to perform numerical calculations which suggest a significant nonlinear reduction in the growth rate.

* tph@mrcabq.com

2 SPREAD-MASS MODEL OF ION-HOSE INSTABILITY

Lee's spread-mass model [2] provides a way to include frequency-spread effects in the equations for transverse motion of the beam and ion-channel centroids: each longitudinal segment of the beam and channel is decomposed into rigid disks having a distribution of mass and labeled by the continuous variables η and ξ ($0 \leq \eta,\ \xi \leq 1$). The centroid of any beam segment ($(\bar{b})$) or channel segment ($(\bar{d})$) is the weighted mean of all the disks; i.e.,

$$\bar{b} = \int_0^1 g(\eta) b_\eta d\eta, \quad \bar{d} = \int_0^1 g(\xi) d_\xi d\xi \tag{1}$$

where $g(x) = 12x^2(1-x)$ is a normalized weighting function appropriate to the Gaussian profile [2]. Making use of Eq. 1 we arrive at the spread-mass model equations for ion-hose oscillations in the presence of a focusing magnetic field. The equations for each rigid disk component are:

$$\frac{\partial^2 b_\eta}{\partial z^2} = -2\eta k_{\beta c}^2 (b_\eta - \bar{d}) + i k_{ce} \frac{\partial b_\eta}{\partial z} \tag{2}$$

$$\frac{\partial^2 d_\xi}{\partial \tau^2} = -2\xi \omega_{\beta i}^2 (d_\xi - \bar{b}) \tag{3}$$

where b and d are complex phasors defined by $b = b_x + i b_y$, $d = d_x + i d_y$, z measures distance along the accelerator and $\tau = t - z/c$ labels a particular beam segment by its time of injection at $z = 0$. The beam betatron wavenumber, cyclotron wavenumber and ion oscillation frequency which appear in the above equations are given respectively by

$$k_{\beta e}^2 = \frac{f\nu}{\gamma R^2}, \quad k_{ce} = \frac{eB_z}{\gamma m_e c^2}, \quad \omega_{\beta i}^2 = \frac{m_e \nu c^2}{m_i R^2} \tag{4}$$

where B_z is the solenoidal focusing magnetic field, m_e and m_i are the electron and ion masses, γ the electron relativistic factor, $\nu = eI_b/mc^3$, f is the fractional neutralization, and R is the RMS beam and channel radius. For a Gaussian beam and channel, the maximum (on-axis) value of the betatron wavenumber (ion frequency) is twice the "rigid beam" value given in Eq. 4, giving rise to the factors of 2 in Eqs. 2 and 3.

We next assume harmonic perturbations for b_η and d_ξ of the form

$$b_\eta, d_\xi \sim e^{i(\omega t - \kappa z)} = e^{i(\omega\tau + kz)} = e^{i(\Omega T + KZ)},$$

where κ is the laboratory wavenumber, $k = \omega/c - \kappa$ is the "Doppler-shifted" wavenumber, and $K = k/k_{\beta e}$ and $\Omega = \omega/\omega_{\beta i}$ are the scaled wavenumber and frequency.

Substitution into Eqs. 2 and 3 and use of the definitions in Eq. 1 results in the dispersion relation

$$\int_0^1 \frac{2\eta\, g(\eta)\, d\eta}{[2\eta - U(K)]} \cdot \int_0^1 \frac{2\xi\, g(\xi)\, d\xi}{[2\xi - W(\Omega)]} = 1 \qquad (5)$$

where $U(K) = K^2 - KK_{ce}$ and $W(\Omega) = \Omega^2$.

To obtain this dispersion relation, we have made the simplifying assumption of constant f. For the case of beam generated ionization, one would expect f at any position z to ramp up roughly linearly with τ. This case is considered in the numerical calculations later in this section and in the simulations of Sec. 3.

Approximating Eq. 5 in the "strong-focusing" limit (where the solenoidal field is the dominant focusing force on the beam), we find that at the end of the accelerator, $z = \ell$, the growth of the instability is bounded according to

$$|\overline{b}| \le Ce^{\Gamma}, \quad \Gamma \approx \frac{4.75 Z_{\max}}{K_{ce}} = \frac{4.75 f \nu m_e c^2 \ell}{e B_z R^2} \qquad (6)$$

A representative set of DARHT-2 parameters is: $I_b = 2$ kA, $\gamma = 25$, $R = 0.5$ cm, $B_z = 830$ G, $\ell = 50$ m, and $p = 2 \times 10^{-7}$ torr. Residual gas analysis of an evacuated DARHT-2 cell showed H_2O to be the dominant species [4]. Making use of the cross section for electron impact ionization of H_2O ($\approx 0.9 \times 10^{-18}$ cm^2 in the range 5–20 MeV) we obtain the following expression for the fractional neutralization f:

$$f \simeq 0.9 \times 10^9 \cdot p(\mathrm{torr}) \cdot \tau(\mathrm{s}) \qquad (7)$$

For the "worst case" assumption that f is constant at its maximum value 3.6×10^{-4} corresponding to $\tau = 2\ \mu$s at the tail of the beam, Eq. 6 gives $\Gamma = 8.26$. Direct numerical solution of Eq. 2 gives a maximum spatial growth $\Gamma = 7.69$ (at $\Omega = \Omega_0 \equiv 1.20$) and we see that the large B_z limit gives a modest overestimate for this parameter set.

Equations 2 and 3 were solved numerically for the above set of parameters, using 50 disks to represent the distribution function $g(x)$. The beam was given a transverse sinusoidal perturbation at $z = 0$ at the normalized resonant frequency Ω_0 (21.6 MHz). The result, curve (a) in Fig. 1, shows that the amplitude of the beam displacement at the end of the accelerator grows over the first few hundred nanoseconds of beam to a steady-state value corresponding to slightly more than seven e-foldings, consistent with the upper bound from the dispersion analysis for a uniform channel. For a linearly ramped channel, we obtain curve (b) of Fig. 1. The instability grows at about the rate given by the analytic dispersion relation if we simply use a value of f equal to its longitudinal average over the length of the accelerator. This seems reasonable, since the pulse-length of 2 μs is much longer than the transit-time through the accelerator (about 170 ns).

The linear theory provides an estimate for the ratio of the amplitudes of the channel and beam displacements. At $\Omega = 1.20$ we find that

$$\frac{|\overline{d}|}{|\overline{b}|} \simeq 4 \qquad (8)$$

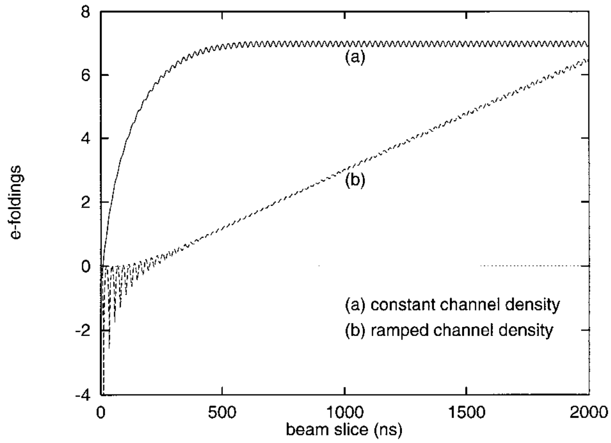

Figure 1: Amplitude of beam displacement at the end of the accelerator ($\ell = 50$ m) for (a) constant channel density and (b) linear ramp channel density. (From numerical integration of linear model equations.)

and this ratio is consistent with the numerical results in the linear regime (cf. Fig. 2). We would expect nonlinear effects to appear for beam-channel displacements of the order of the radius R, and in light of Eq. 8, for beam displacements as small as perhaps 10–20% of the radius. Replacing the linear beam-channel restoring forces in Eqs. 2 and 3 with a nonlinear term [3], we obtained the results shown in Fig. 2, where linear growth of the beam displacement stops at a level slightly below 10% of the radius R. Calculations at several other pressures further suggest that the saturation level is roughly proportional to the pressure and hence to the linear growth rate. These conclusions were investigated more quantitatively in a series of numerical simulations described in the following section.

3 SIMULATIONS OF ION-HOSE INSTABILITY

The spread-mass model presented above is based on a simplified model of beam dynamics. To check the results it gives, and include some additional effects, we have used the particle-in-cell code LSP [5]. For this problem, LSP calculates the transverse electric and magnetic fields from Poisson-type equations, which are solved using 2-D FFT's. Particles are pushed in the transverse direction using the Lorentz equation.

We first carried out a series of benchmark calculations to compare the PIC model with the spread-mass model. The beam energy was constant (no acceleration) and a constant axial magnetic field was used. The physical parameters were: $\gamma = 25$, $I_b = 2$ kA, $R = 0.5$ cm, $\epsilon_L = 0.1$ cm-rad, $B_z = 830$ gauss, $\ell = 50$ m. Six simulations were carried out, with vacuum pressures from 10^{-7} to 6×10^{-7} torr. For a pressure of 6×10^{-7} torr, the transverse beam and channel displacement at the end of the 50 m drift space

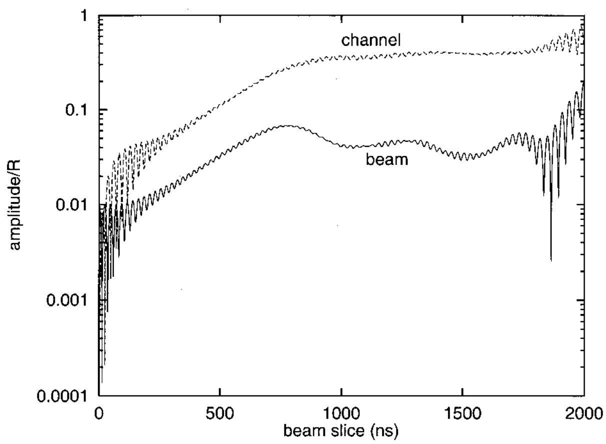

Figure 2: Amplitude of the beam and channel displacements (in units of the beam radius R) from numerical integration of the nonlinear model equations for same parameters as in Fig.1.

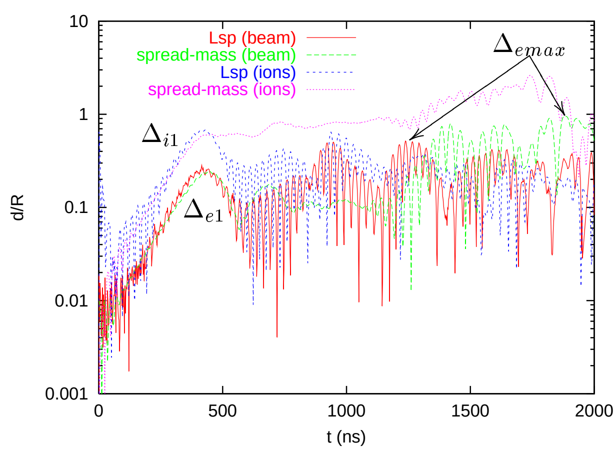

Figure 3: Comparison of centroid displacements at end of drift-space from 3-D PIC simulation and spread-mass models for a pressure of 6×10^{-7} torr.

are plotted in Fig. 3. The agreement between the spread-mass and PIC models is quite good in the linear regime and early nonlinear regime. In Fig. 4, we compare three values of the centroid amplitude at the end of the drift space from the two models: the beam and ion centroids at the first nonlinear peak (Δ_{e1} and Δ_{i1} in Fig.3), and the beam centroid at the maximum peak, wherever in the pulse it occurs (Δ_{emax} in Fig. 3).

The poorer agreements in the later nonlinear stages is perhaps not surprising since the spread-mass model may not capture the nonlinear changes in the beam distribution.

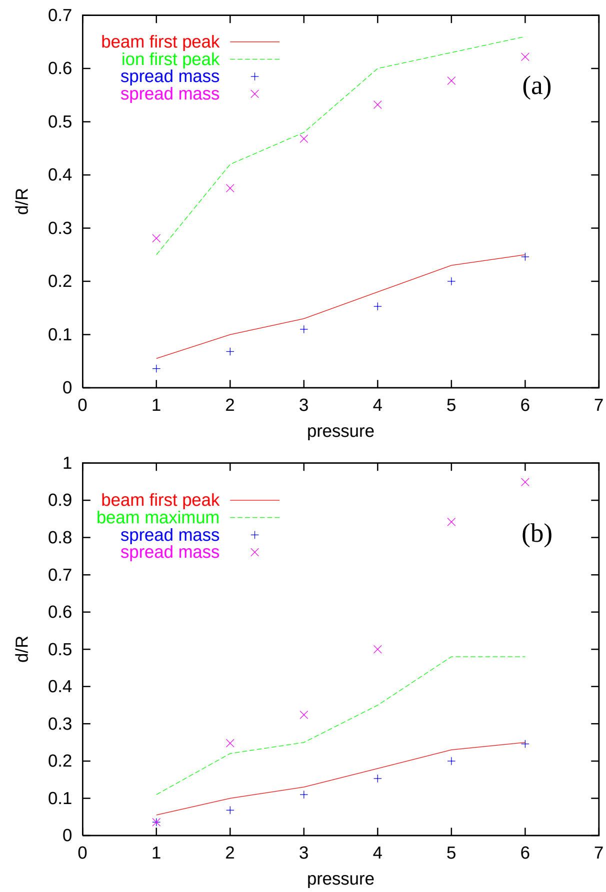

Figure 4: Comparison of centroid displacements at end of drift-space from PIC and spread-mass models vs. pressure (units of 10^{-7} torr). Plot (a) compares the first nonlinear peak for the beam (Δ_{e1}) and ions (Δ_{i1}). Plot (b) shows the first (Δ_{e1}) and maximum (Δ_{emax}) peaks for the beam.

4 ACKNOWLEDGMENTS

This work was motivated by a calculation due to R. J. Briggs. We thank Dr. Daniel Prono for useful discussions. The work was supported by Los Alamos National Laboratory.

5 REFERENCES

[1] M. J. Burns, et al., paper WOAA008, this meeting.

[2] E. P. Lee. Resistive hose instability of a beam with the Bennett profile. *Phys. Fluids*, 21(8):1327, 1978.

[3] H. L. Buchanan. Electron beam propagation in the ion-focused regime. *Phys. Fluids*, 30(1):221, 1987.

[4] D. Prono, private communication, 2000.

[5] Lsp is a software product of Mission Research Corporation (http://www.mrcabq.com).